

**Zeitschrift:** Helvetica Physica Acta  
**Band:** 58 (1985)  
**Heft:** 2-3

**Artikel:** Oscillation mechanics in the assessment of airflow obstruction : from physical principles to clinical investigations  
**Autor:** Depeursinge, C.D. / Perret, C.H.  
**DOI:** <https://doi.org/10.5169/seals-115618>

#### **Nutzungsbedingungen**

Die ETH-Bibliothek ist die Anbieterin der digitalisierten Zeitschriften auf E-Periodica. Sie besitzt keine Urheberrechte an den Zeitschriften und ist nicht verantwortlich für deren Inhalte. Die Rechte liegen in der Regel bei den Herausgebern beziehungsweise den externen Rechteinhabern. Das Veröffentlichen von Bildern in Print- und Online-Publikationen sowie auf Social Media-Kanälen oder Webseiten ist nur mit vorheriger Genehmigung der Rechteinhaber erlaubt. [Mehr erfahren](#)

#### **Conditions d'utilisation**

L'ETH Library est le fournisseur des revues numérisées. Elle ne détient aucun droit d'auteur sur les revues et n'est pas responsable de leur contenu. En règle générale, les droits sont détenus par les éditeurs ou les détenteurs de droits externes. La reproduction d'images dans des publications imprimées ou en ligne ainsi que sur des canaux de médias sociaux ou des sites web n'est autorisée qu'avec l'accord préalable des détenteurs des droits. [En savoir plus](#)

#### **Terms of use**

The ETH Library is the provider of the digitised journals. It does not own any copyrights to the journals and is not responsible for their content. The rights usually lie with the publishers or the external rights holders. Publishing images in print and online publications, as well as on social media channels or websites, is only permitted with the prior consent of the rights holders. [Find out more](#)

**Download PDF:** 10.01.2026

**ETH-Bibliothek Zürich, E-Periodica, <https://www.e-periodica.ch>**

# Oscillation mechanics in the assessment of airflow obstruction: from physical principles to clinical investigations

By C. D. Depeursinge and C. H. Perret\*

Institute of Applied Physics, Federal Institute of Technology,  
1015 Lausanne, Switzerland and \*Institute of Pathophysiology,  
University of Lausanne, 1011, Lausanne, Switzerland

(1. XII. 1984)

In honor of Emanuel Mooser's 60th birthday

**Abstract.** Airflow limitation is a common characteristic of a large number of acute and chronic pulmonary diseases. The measurement of the acoustical impedance of the respiratory system provides new quantitative data in the assessment of airway obstruction. A physical model is presented, in which the morphological as well as rheologic data of the lung are taken into consideration. Bronchial walls are supposed to possess elastance, resistance and inertance. As far as possible, physical properties of gases are included in the calculation: viscosity, inertia, compressibility and thermal losses. Flow entrance effects and non-linear phenomena are, however, ignored. Computation of the acoustical impedance of the lung has been carried out for a self-consistent, symmetrically and asymmetrically branching duct network. Results are found to be in fair agreement with experimental results. The effects of a simulated peripheral bronchoconstriction are presented. The simulation provides, in particular, a good understanding of the bronchodilator action in asthmatic patients.

## 1. Introduction

### 1.1. *The problem of airway obstruction from a medical point of view*

Respiratory diseases account for up to eleven per cent of the total cost of ambulatory medicine and twelve per cent of all pharmaceutical expenses. In Switzerland, this represents several million Swiss francs every year [1, 2, 3]. The pathologic processes involved affect mainly lung parenchyma and airways. At an earlier or later stage of the disease, they manifest themselves as an airway obstruction.

Airflow obstruction may be defined as an inability to expel a normal proportion of the total lung volume in a given time. Airflow limitation is a common characteristic of the chronic obstructive pulmonary disease: chronic bronchitis, in which the bronchi are narrowed by inflammation, emphysema, in which the walls of some of the small airways are damaged, and brochial asthma, in which the muscles in the walls of some bronchi constrict. At an early stage of the disease, breathlessness occurs during exercise only, when the ventilatory demand exceeds the respiratory response. At a final stage, or during exacerbation of the disease, severe breathlessness may be present, even at rest.

Deleterious effects of smoking or environmental factors, such as pollution, allergens and some particular occupational conditions, must be detected early. Mild airway obstruction may be detected by appropriate lung function tests. Bronchial challenge may reveal bronchial asthma. These investigations require expensive equipment and active cooperation from the patient.

The forced oscillation techniques have proved to provide meaningful information on pulmonary mechanics [4]. The acoustical respiratory impedance measurement is easy to perform, fast and noninvasive. For that reason, it is of great interest for lung function tests in small children, bronchial challenge and for acute asthmatic attack or cardiac failure in critically ill patients.

## 1.2. *The problem of airways obstruction from the physical principles*

In spite of a large number of works devoted to fluid mechanical calculations of airway resistance, much remains to be understood in order to get a proper evaluation of the physiologic and pathophysiologic observations. Future efforts in pulmonary fluid dynamical studies are likely to be very profitable in the search for discriminating diagnostic tests. It is commonly admitted that no test is yet available that can clearly diagnose lung disease at an early stage, before symptoms appear. The difficulties in a fluid mechanical approach of the problem of bronchial obstruction arise on one hand from the complexity and variability of the anatomical structures, on the other hand from the rheologic aspects of the lung tissues.

The case of quasi-steady flow in airways has been well reviewed by Pedley et al. [5]. The flow patterns in the branching network have been studied both theoretically and experimentally. turbulent flow is observed in the trachea at Reynolds numbers  $Re$  around 3000 (flow rate =  $0.67 \text{ l s}^{-1}$ ). For rapid breathing patterns,  $Re$  values may climb well above 10000. It is however argued by Pedley, Schroeter and Sudlow [6] that the presence of turbulences will not affect significantly the pressure drop for  $Re$  values lower than 10000. When flowing towards smaller airways, air speed slackens because of the large increase in the total cross-sectional area after the eighth or ninth generation. When bronchi have a diameter of approximately 2 mm:  $Re$  numbers fall below 50. In the terminal airways,  $Re$  is close to one. Pressure drop in this case is largely proportional to the flow rate and dominated by viscous losses. The Hagen-Poiseuille law for laminar flow is however not valid, even in this case, since the entrance length, i.e. the distance necessary to reestablish Poiseuille flow after disturbance, is longer than a single airway segment: Poiseuille flow is therefore never fully established.

Fewer studies have been devoted to the problem of unsteady flow in airways. Spontaneous respiration is essentially an oscillatory process and therefore unsteady in nature. Furthermore, various stimulations, for instance of cardiac or muscular origin reinforce the unsteady character of the airflow. When rapidly changing pressure gradients are considered, the nature of the flow may be radically changed by the increase of the inertial contribution to the pressure drop. Dynamical fluid equations must be reconsidered from scratch. This is true, in particular, when the response of the lung to high frequency pressure oscillations (0–50 Hertz) must be understood. Quite complex phenomena take place, which must be taken into account and described. A phenomenological approach must be adopted.

### 1.3. *Functional identification*

Functional identification of the lung-thorax system can be achieved by a stimulus-response experiment: in the so called 'forced oscillation technique' [7] or 'forced excitation technique', a pressure signal is applied to the mouth and acts as a stimulus. If the airflow induced by the pressure varies approximately linearly, the functional relationship between the stimulus and the response can be described by a transfer function, which is, in this particular case, the acoustical impedance of the lung-thorax system. This transfer function is usually estimated in the frequency domain. Most of the early experiments have been performed with sinusoidal excitation at a single frequency or at a limited number of frequencies.

Non-sinusoidal stimulations have been used in later experiments. Signals containing all the frequencies of interest allow a rapid determination of the impedance by spectral analysis of input and output signals. The use of random noise excitation presents further advantages: Gaussian white noise stimulation yields the most comprehensive input signal to the tested system and allows, in particular, a determination of non-linear effects. The set of Wiener kernels achieves a complete characterisation of the dynamic mechanical behaviour of the lung-thorax system [8].

This 'black box' approach ignores, however, the mechanisms underlying the dynamic response of the lung-thorax system. One could expect a better understanding of the stimulus-response relationship by decomposing the physiological system into its ultimate components.

### 1.4. *Structural identification*

The structural identification of the lung-thorax system aims at analysing the response of the various anatomical parts and their interactions. From morphometric studies, the airways appear as a complex asymmetrically branching network of ducts with yielding walls, leading to the alveolar sacs. In addition to the structure of the lung itself, upper airways including glottis and susglottal structures, as well as the thoracic cage, must also be considered.

In the vast majority of published works, impedance data are interpreted using linear, lumped parameter models with elements representing resistive, inertial and compliant effects. The simplest model of this sort is the three-element-model with one resistance, one inertance and one compliance in series. In healthy subjects it yields, 'by chance', an acceptable description of the frequency dependence in the range 4–30 Hz. It, however, fails to explain correctly the impedance data in subjects with lung disease. The estimation of the parameters involved in more complex algorithms must be developed to fit experimental data. It must be suspected that in some cases, electrical analog lumped models, built up with frequency invariant components, could act as misleading aids in the understanding of experimental data. Solving fluid mechanical equations leads to frequency dependent resistive and inertial components and the use of fixed value components appears unwarranted from a physical point of view.

The calculation of the acoustical response of a complex branching duct network, featuring the bronchial tree, has been reported in a limited number of papers. Fredberg et al. [9, 10, 11, 12] have proposed to compute the acoustical

impedance of a complex asymmetrically branching network of ducts with yielding walls. Similar calculations have been performed by Winter et al. [12] in order to compare experimental data and theoretical predictions for the frequency dependence of the phase velocity in the trachea of the dog.

The impedance computed in a low frequency range for a symmetrically and asymmetrically branching duct network is presented in this paper. In particular, the effect on impedance data of a simulated peripheral bronchoconstriction is shown.

## 2. Method

The total impedance of the lung has been computed as the resultant of the individual impedances of each bronchial segment. Individual links in the bronchial tree are modelled as cylinders of constant cross section. The cylinder walls are supposed to possess elastance, inertance and resistance. Entrance effects, possible turbulences have been ignored in a first approach. Computation has been performed at the limit of low fluid velocities in order to avoid non linear phenomena.

### 2.1. Impedance of a long, straight elastic tube

A cylindrical section of an infinite straight elastic tube is schematized on Fig. 1. The fluid velocity vector is decomposed in a cylindrical coordinate reference frame. The Navier-Stokes equations for the airflow in a long straight tube can be linearized under the following assumptions:

- the flow is treated as one-dimensional: the radial and transverse components of the velocity are neglected.
- only small variations of velocity, pressure and therefore of gas density are considered.

Under these assumptions, the Navier-Stokes equations can be written for the axial velocity  $u$  and pressure  $p$  in the following way:

$$\frac{\partial^2 u}{\partial r^2} + \frac{1}{r} \frac{\partial u}{\partial r} - \frac{1}{\nu_0} \frac{\partial u}{\partial t} = \frac{1}{\mu} \frac{\partial p}{\partial t} \quad (1)$$

( $\nu_0$ : kinematic viscosity,  $\mu$  dynamic viscosity)

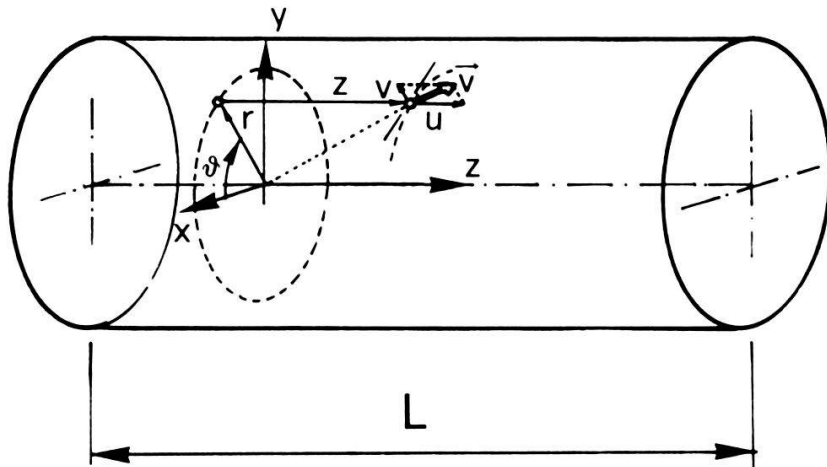


Figure 1

Section of a long straight tube. The velocity  $V$  is represented by its cylindrical coordinate components:  $u$  longitudinal and  $v$  radial component.

An exact solution can be found in the form:

$$U = -\frac{\nu_0}{\mu} \frac{1}{i\omega} \left( 1 - \frac{J_0(\alpha y e^{3i\pi/4})}{J_0(\alpha e^{3i\pi/4})} \right) \quad (2)$$

where  $U$  is the Fourier representation of  $u$ :  $u = U e^{i\omega t}$   $\omega$ : pulsation,  $J_0$  Bessel function of order zero,  $\alpha$  is the Womersley parameter:

$$\alpha = \sqrt{\frac{\omega}{\nu_0}} R \quad (3)$$

and  $y = r/R$  where  $R$  is the radius of the tube and  $r$  the radial coordinate.

From the solution of Navier-Stokes equation (1), one can derive a partial differential equation between airflow  $q$  and pressure  $p$  (Fourier representations:  $q = Q e^{i\omega t}$  and  $p = P e^{i\omega t}$ ) in the form:

$$I_s \frac{\partial q}{\partial t} + R_s q = -\frac{\partial p}{\partial z} \quad (4)$$

This equation, where  $I_s$  and  $R_s$  are the inertance and resistance per unit length, typically evokes an acoustical distributed line with a serial impedance  $Z_s$  per unit length. In Fourier representation:

$$Z_s Q = -\frac{\partial P}{\partial z} \quad (5)$$

with:

$$Z_s = \frac{\mu}{\nu_0 S_0} i\omega \left[ 1 - \frac{2J_1(\alpha e^{3i\pi/4})}{\alpha e^{3i\pi/4} J_0(\alpha e^{3i\pi/4})} \right]^{-1} \quad (6)$$

( $S_0$ : section of the tube,  $J_1$ : First order Bessel function).

The serial resistance  $R_s$  and reactance  $I_s$  are plotted as a function of frequency in Fig. 2 for a tube with radius  $R = 11$  mm which is consistent with upper airway

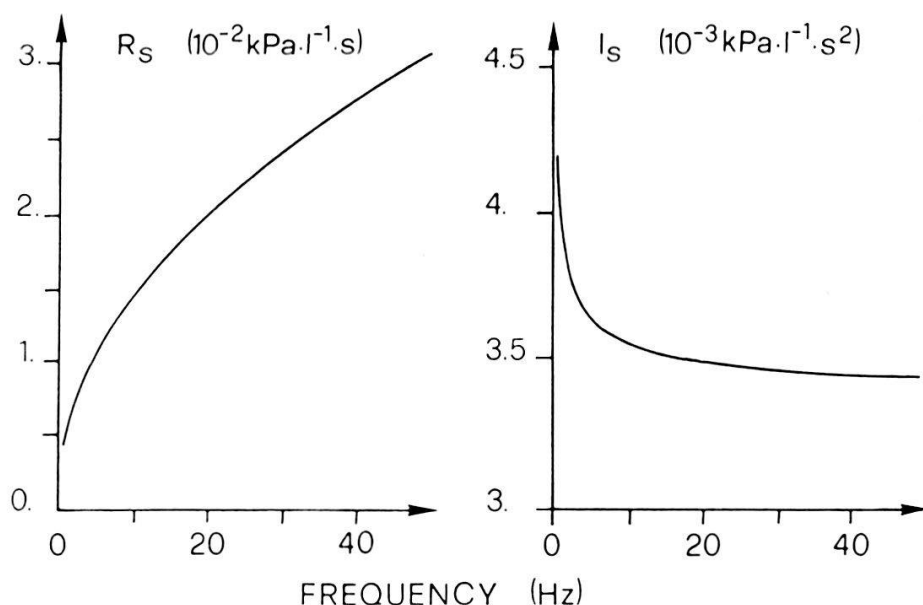


Figure 2

Frequency dependence of the serial resistance  $R_s$  and serial inertance  $I_s$ , for a 22 mm diameter tube section of unit length (1 m)

dimensions. A strong dependence of  $R_s$  with frequency is observed. This result contrasts with the frequency independence implicitly assumed by investigators who invoke electrical analogs to explain the modifications of the impedance curves with frequency.

The parallel admittance per unit length describes the gas compression and thermal losses from the gas to the wall. The temperature distribution ( $T$ ) in the fluid can be computed from a local energy balance equation:

$$k \Delta T - \rho c_v \frac{\partial T}{\partial t} = p \frac{\partial u}{\partial z}, \quad (7)$$

( $\rho$ : gas density,  $c_v$ : specific heat at constant volume)

( $k$ : thermal conductance of the gas)

where the mechanical work  $p \cdot (\partial u / \partial z)$  can be computed from the continuity equation:

$$\frac{\partial u}{\partial z} = -\frac{1}{\rho} \frac{\partial p}{\partial t}, \quad (8)$$

and the state equation in the form:

$$p = \frac{R}{M} \rho T \quad (9)$$

( $R$ : gas constant,  $M$ : molar mass)

The importance of the thermal characteristics of the tube wall has been evaluated by different authors [13, 14]. The temperature  $T_w$ , in the wall is computed from:

$$k_w \Delta T_w - \rho_w c_w \frac{\partial T_w}{\partial t} = 0 \quad (10)$$

( $k_w$ : thermal conductance of the wall,  $\rho_w$  wall density,  $c_w$ : specific heat of the wall)

After resolution of both temperature equations with appropriate boundary conditions, a precise expression can be obtained for the temperature distribution of the gas:

$$\Theta = \frac{P}{\rho c_p} \left[ 1 - \frac{J_0(\alpha_g y e^{3i\pi/4})}{J_0(\alpha_g e^{3i\pi/4}) - i A J_1(\alpha_g e^{3i\pi/4})} \right]. \quad (11)$$

( $c_p$ : specific heat of the gas at constant pressure)

$\Theta$  is the Fourier representation of the temperature distribution  $T = \Theta e^{i\omega t}$ , and:

$$A = \sqrt{\frac{\rho_0 k c_p}{\rho_w k_w c_w}}.$$

In order to get a comprehensive expression of the parallel admittance, the yielding character of the bronchial wall must be considered.

Figure 3a schematizes a section of an elastic tube. The fluid balance in the

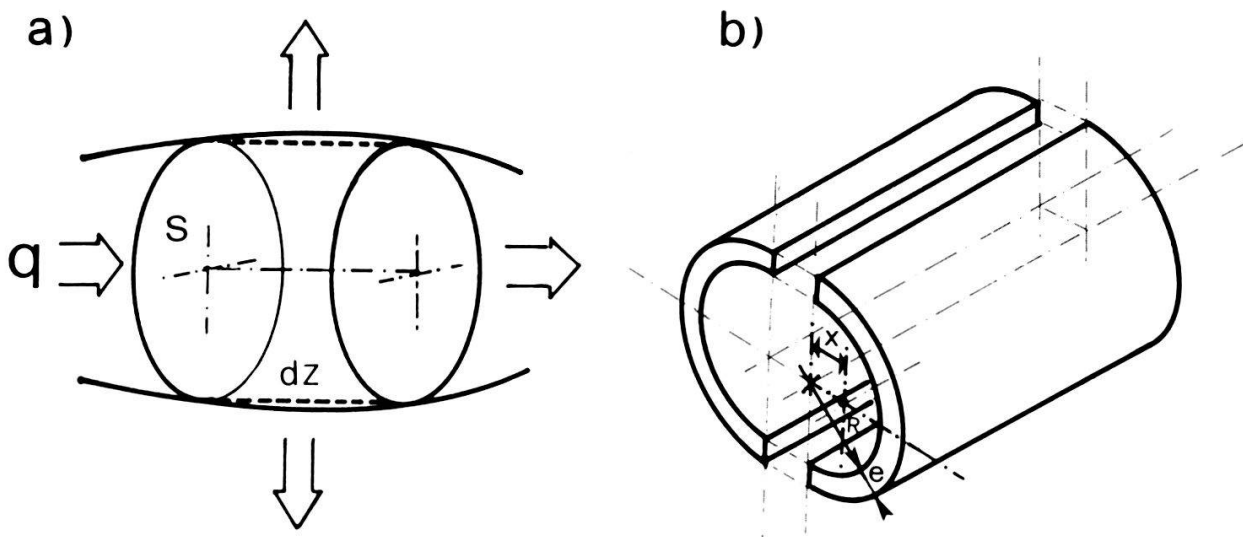


Figure 3

a) Section of an elastic tube with arrows representing the different terms in the fluid balance equation.  
 b) Half section of a bronchi considered for the calculation of wall elastance and inertance. See text for symbols.

yielding wall tube can be expressed in the following way:

$$\frac{\partial q}{\partial z} dz + \frac{\partial s}{\partial t} dz = -\frac{S_0}{\rho} \frac{\partial p}{\partial t} dz \quad (12)$$

( $s$ : tube section)

The first left hand term represents the longitudinal balance of the fluid whereas the second left hand term accounts for the lateral flow. The right hand term accounts for gas compression and can be computed from the continuity and state equation:

$$-\frac{1}{\rho} \frac{\partial p}{\partial t} = -\frac{1}{p_0} \frac{dp}{dt} + \frac{1}{T_0} \frac{d\langle T \rangle}{dt} \quad (13)$$

( $p_0, T_0$ : equilibrium pressure and temperature)

$\langle T \rangle$  is the temperature averaged over the tube section and can be calculated from (11) by integration over the section of the tube.

To evaluate the elastance and inertance of the bronchial wall, a segment of bronchi, divided into two parts along its axis, has been considered (Fig. 3b). Assuming, in first approximation, a linear relationship between deformation and stress for small pressure variations around  $p_0$  a proportionality can be established between the instantaneous pressure and the bronchial section variations  $s - s_0$

$$k_w = \frac{p - p_0}{s - s_0} = \frac{1}{2} \frac{Ee}{R} \quad (14)$$

$k_w$  is the wall elastance. It varies as the ratio  $e/R$  of the bronchial thickness to the radius  $R$ , if the variations of Young's modulus  $E$  over the different bronchial links are assumed to be small.  $k_w$  is therefore not expected to change too much along

the bronchial tree.  $k_w$  will be derived from the published works on the large bronchi.

Similarly the bronchial wall inertance can be estimated from Newton's equation written for the bronchial half section with unity length:

$$\frac{1}{2}W_w \frac{d^2x}{dt^2} = 2R(p - p_0) \quad (15)$$

where  $w_w$  is the weight of the bronchial segment and

$$x = \frac{2}{3\pi} \frac{(R + e)^3 - R^3}{(R + e)^2 - R^2} \quad (16)$$

is the abscissa of the center of mass. After elimination of second order terms, (15) may be written in the form:

$$M_w \frac{1}{S_0} \frac{d^2s}{dt^2} = p - p_0 \quad (17)$$

with

$$M_w = \frac{\rho_w S_0 e}{2\pi R} = \frac{W_w}{4\pi} \quad (18)$$

$M_w$  is the specific wall inertance. It varies as the section  $S_0$  of the bronchial segment. The dynamic response of the wall can therefore be modelled as a second order local oscillator:

$$\frac{1}{S_0} \left( M_w \frac{d^2s}{dt^2} + D_w \frac{ds}{dt} + K_w \right) = p - p_0 \quad (19)$$

In Fourier representation:

$$\frac{S}{S_0} = \frac{p}{-\omega^2 M_w + i\omega D_w + K_w} \quad (20)$$

From (19) and (20):

$$\frac{\partial q}{\partial z} = -\frac{S_0}{p_0} \frac{dp}{dt} + \frac{S_0}{T_0} \frac{d\langle T \rangle}{dt} - \frac{\partial s}{\partial t}, \quad (21)$$

which must be put in the form

$$-\frac{\partial q}{\partial z} = C_p \frac{\partial p}{\partial t} + G_p p \quad (22)$$

which is the second partial derivative equation describing the propagation of the pressure and flow wave along the bronchial tree.  $C_p$  is the parallel compliance and  $G_p$  the parallel conductance. In the Fourier representation; (22) can be written:

$$-\frac{\partial Q}{\partial z} = i\omega C_p P + G_p P = Y_p P \quad (23)$$

where  $Y_p$  is the parallel admittance. From (23):

$$Y_p = \frac{-(\partial Q/\partial z)}{p} = Y_{pr} + Y_{pe} \quad (24)$$

$Y_{pr}$  is the parallel admittance of the tube with rigid walls. From (21):

$$Y_{pr} = i\omega S_0 \left( \frac{1}{p_0} - \frac{1}{T_0} \frac{\langle \Theta \rangle}{p} \right) = \frac{S_0}{\gamma' p_0} i\omega \left[ 1 + \frac{2(\gamma' - 1)(\alpha_g e^{3i\pi/4})}{\alpha_g e^{3i\pi/4} (J_0(\alpha_g e^{3i\pi/4}) + iA J_1(\alpha_g e^{3i\pi/4}))} \right] \quad (25)$$

$$(\gamma' = c_p/c_v)$$

and  $Y_{pe}$  is the parallel admittance of the tube with yielding walls and filled with an incompressible fluid.

$$Y_{pe} = i\omega S_0 \left( \frac{S/S_0}{p} \right) = \frac{i\omega S_0}{-\omega^2 M_w + i\omega D_w + K_w} \quad (26)$$

Finally, the impedance of a bronchial segment of length  $L$  is computed from:

$$Z = Z_0 \frac{Z_0 t h \gamma L + Z_L}{Z_0 + Z_L t h \gamma L} \quad (27)$$

Where  $Z_0$  is the characteristic impedance of the duct:

$$Z_0 = \sqrt{\frac{Z_s}{Y_p}} \quad (28)$$

and the propagation constant:

$$\gamma = \sqrt{Z_s \cdot Y_p} \quad (29)$$

$Z_L$  is the load impedance at the extremity of the bronchial segment.

## 2.2. Impedance of a branching duct network

The lung airways form a complex system of branching tubes whose diameters decrease from the trachea to the terminal bronchioles. The airways divide regularly from the trachea to the alveolar sacs: 23 generations have been observed, which yield a total number of about 16 million interconnected ducts in the bronchial tree [16]. The computation of the resulting impedance therefore appears as a gigantic task. The use of the concept of self consistency introduced by Fredberg [9] allows a drastic reduction of the computational task. This concept is based on two simplifying assumptions:

First, the lung is supposed to be homogeneous. The impedances of the terminal bronchioles are assumed to be equal. This assumption simplifies considerably the computation of the impedance of a structurally symmetric duct network. The symmetric model is, however, far from reality. An asymmetric branching duct network has been proposed by Horsefield and Cumming [17]. The airway links are numbered in increasing order from the terminal bronchioles

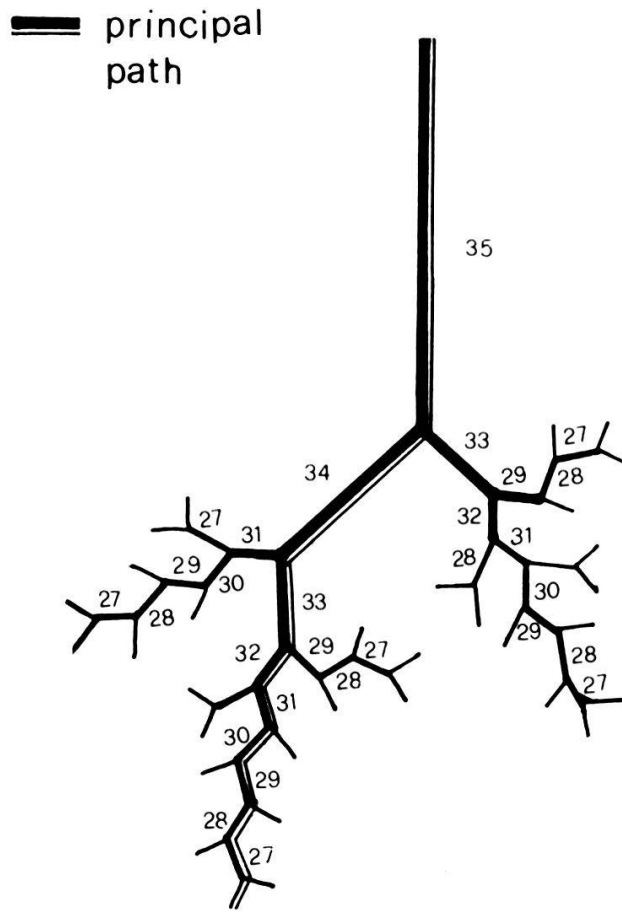


Figure 4

Schematic diagram of an asymmetrically branching duct network. Examples of Horsefield orders are given for the first nine generations.

towards the trachea: this is the Horsefield order. An example of an asymmetric bronchial tree is shown in Fig. 4.

The second simplifying assumption can be formulated as follows [9]: In an asymmetric self-consistent network, an airway link input impedance is a unique function of its Horsefield order. The computer program has therefore been developed in a simple way: the input impedances are computed along the principal path, i.e. along the longest path in the bronchial tree. For each bronchial link, the load impedance  $Z_L$  is calculated as the parallel combination of the impedances of the ducts with Horsefield orders  $(n - 1)$  and  $(n - i(n))$  where  $i(n)$  is greater or equal to 1:

$$Z_L^{-1}(n) = Z^{-1}(n - i(n)) + Z^{-1}(n - 1) \quad (30)$$

The values of  $Z_L$  are recursively calculated at each node of the bronchial tree. The recursion index  $i(n)$  is derived from the morphometrical data published by Horsefield and Cumming [17]. In this computation, the entrance effects have been neglected. This assumption remains to be proved. It stems from the fact that oscillatory flow rapidly becomes uniform over the bronchial section, both in phase and amplitude. Perturbations of the flow patterns in long tubes are therefore expected to be much smaller in unsteady flows than in quasi steady flows.

### 3. Results

Morphometric data have been taken from ref. [9], for the symmetrically and asymmetrically branching duct network. These data have been derived from the

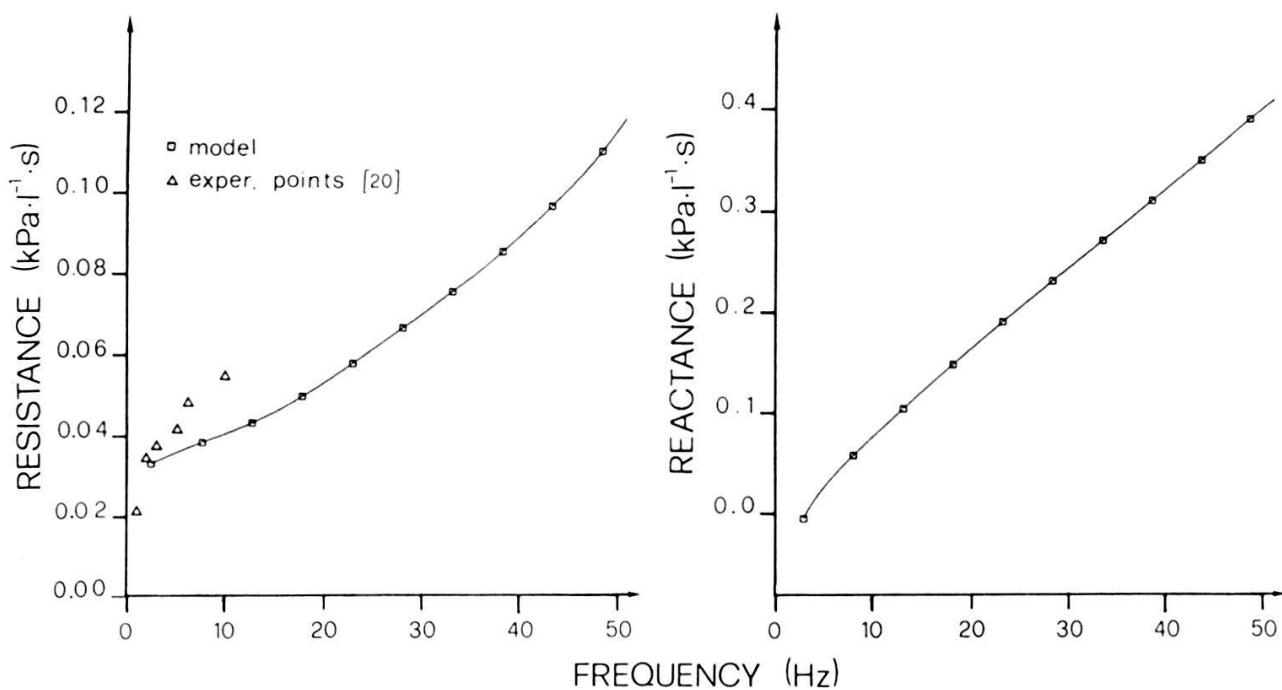


Figure 5

Resistance and reactance curves computed for our physical model of the lung. Experimental data from Finucane et al. [20] are plotted for comparison.

structurally symmetric Weibel morphology [16] and from the description given by Horsefield and Cumming of the asymmetric regular tree [17]. The choice of the terminal link impedance boundary conditions is critical for a proper evaluation of the influence on the respiratory impedance of bronchial obstruction.

It is implicitly assumed that alveolar sacs are homogeneously influenced by thoracic strain. The compliances at the terminal links have been calculated as the total lung compliance divided by the number of terminal links ( $8.38 \times 10^6$  and  $6.81 \times 10^6$  for the symmetric and asymmetric tree). Lung compliance can be estimated on the basis of published data [18, 19]. A typical value of  $0.021 \text{ kPa}^{-1}$  has been chosen in accordance with Fredberg [9]. Data for the terminal link resistance and reactance are not available in the literature. Values for the lung resistance  $R_L$  and lung elastance  $E_L$  are found in Refs [18] and [19], but they include the contribution of the bronchial tree itself. In particular, the values taken by Fredberg [9] for the lung tissue resistance  $R_T$  and the lung tissue inertance  $I_T$  appear largely overestimated. The result of the computation in a 0 to 50 Hz range is presented on Fig. 5. The resistance and reactance curves have been calculated for  $C_T = 21 \text{ kPa}^{-1}$ ,  $I_T = 0.0001 \text{ kPa l}^{-1} \text{ s}^2$  and  $R_T = 0.015 \text{ kPa l}^{-1} \text{ s}$ . Higher values of  $I_T$  give rise to a resonance in the 0 to 50 Hz range. The associated peak of the resistance is never observed experimentally. The resistance value typically obtained by Finucane [9] in a healthy subject are reported on the resistance diagram of Fig. 5.

Figure 6 illustrates the modifications of the resistance and reactance curves of the lung, when a peripheral bronchoconstriction is simulated: the diameter of each bronchial link of the branching duct network has been diminished by subtracting a given value ranging from  $130 \mu\text{m}$  to  $180 \mu\text{m}$ . The resistances of small airways are strongly increased in comparison with the resistances of large airways which are almost unaffected by the reduction of their diameter. For a mild, increasing peripheral obstruction, the resistances are evenly raised in the

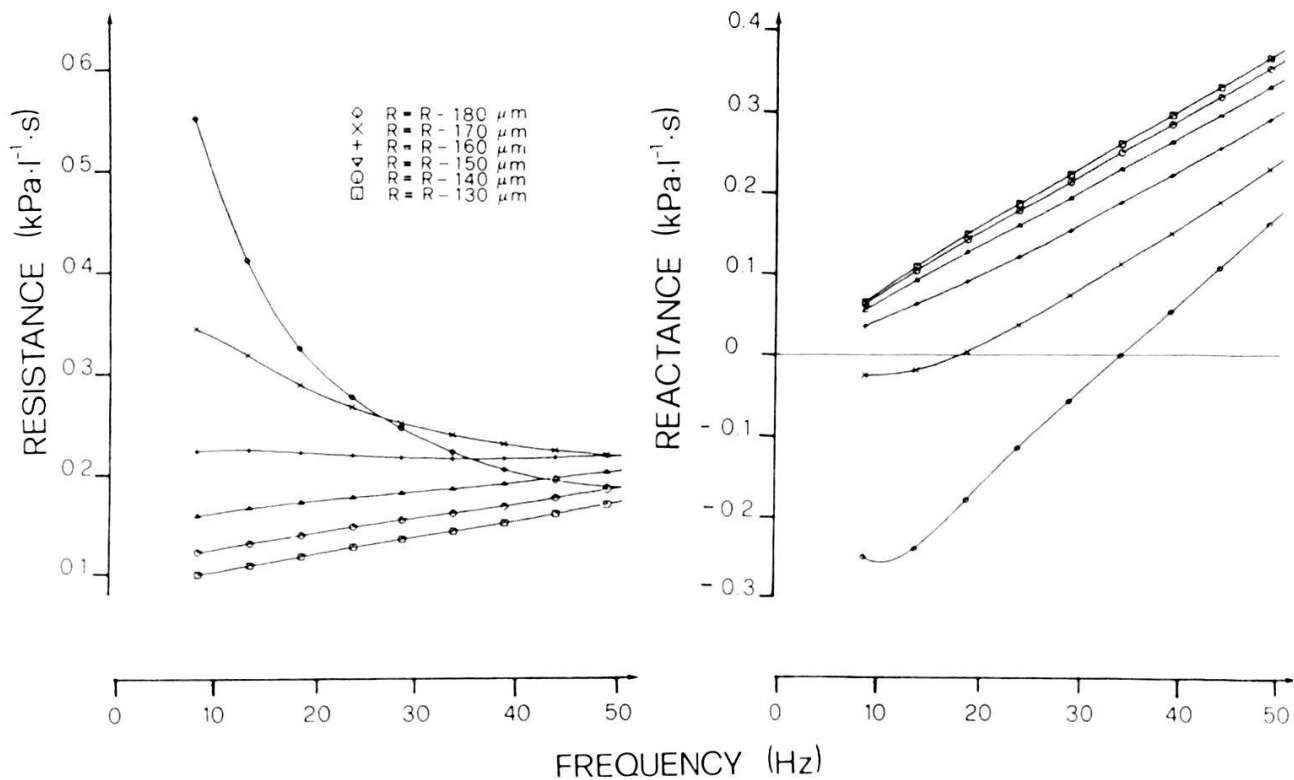


Figure 6  
Effect on the resistance and reactance curves of a simulated peripheral bronchoconstriction. Computed impedance curves are shown for bronchial radius reductions ranging from 130  $\mu\text{m}$  to 180  $\mu\text{m}$ .

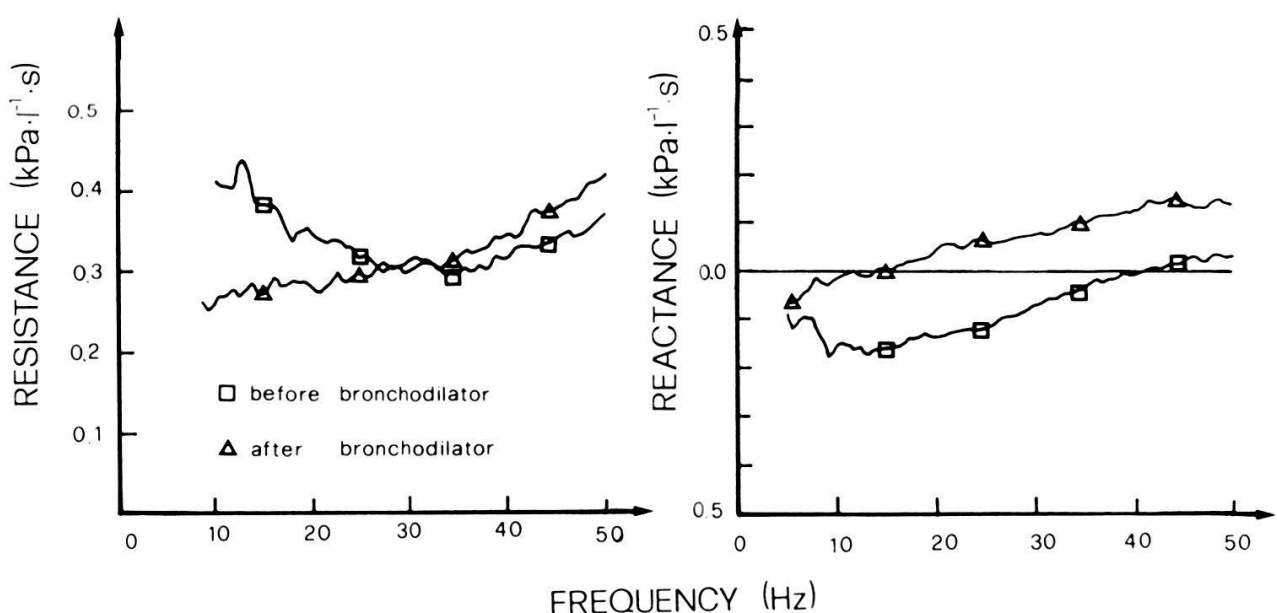


Figure 7  
Resistance and reactance curves measured experimentally in an asthmatic patient, before and after administration of a bronchodilatator.

frequency interval and the reactances are slightly lowered. This decrease is more pronounced at high frequencies. When the peripheral bronchoconstriction is more severe, a characteristic rise in the resistances at low frequencies is observed, giving rise to the typical 'cuvette' shaped curve. The reactances are lowered over the whole frequency range. These modifications of the resistance and reactance curves, predicted from the model, agree perfectly with the results of measurements in obstructive patients: Fig. 7 shows the resistance and reactance curves measured in an asthmatic patient before and after administration of a bronchodilator. Before medication, a pronounced rising of the resistance at low frequencies is obvious. It suddenly disappears after bronchodilation, giving way to a monotonous increase of the resistance with frequency. The reactances, initially strongly negative, increased markedly after administration of the bronchodilator.

#### 4. Discussion

Morphometric data involved in the computation of the acoustical impedance have been derived from Weibel's model of a symmetric lung [16]. These data are known to correspond to lung volumes equal to 75% of the total lung capacity (TLC). The results of the calculation of the impedance of the symmetrically and asymmetrically branching duct networks are in fair agreement with experimental data reported by Finucane at 80% of TLC. The slight increase in resistance with frequency between 1 and 10 Hz has been explained by this author as reflecting the changes in the distribution of flow with frequency. The experimental results of Finucane have been further discussed by Fredberg and Mead [10], on the basis of a distributed parameter model of the tracheobronchial tree, similar to the model presented in this article. The conclusions of these authors are that only half of this resistance increase can be explained by changes in the distribution of flow among parallel inhomogeneities, the second half being mainly due to the distortion of velocity profiles caused mainly by inertial terms, then to the changes in the flow distribution along the tube caused by gas compliance and finally, to bronchial wall compliance. Our results deviates from the analysis of Fredberg et al. on the following points:

Our model yields unrealistic impedance values for the terminal link impedance boundary conditions selected by Fredberg [9]. In particular, a tissue resistance of  $0.05 \text{ kPa l}^{-1} \text{ s}$  give rise, in our model, to impedance curves which are typically observed in obstructive patients. This result suggests that the tissue resistances, without the contribution of airflow viscous resistances, are much smaller.

For a total tissue resistance  $R_T$  of  $0.015 \text{ kPa l}^{-1} \text{ s}$ , a total alveolar compliance  $C_T$  of  $21 \text{ kPa}^{-1}$  and a lung tissue inertance  $I_T = 0.0001 \text{ kPa l}^{-1} \text{ s}^2$ , which is five times lower than the value taken by Fredberg [9], our model yields impedance curves in good agreement with experimental data [20]. At frequencies higher than 10 Hz, the 'in vivo' measurement of lung impedance, without the contribution from the thoracic cage nor the upper airways, are not available at present. Impedance data in excised human lung have been published by Van Brabandt et al. [19]. Total lung resistances are found to be significantly higher than the lung resistances measured in healthy subjects and predicted by our model. This discrepancy must be attributed to lower lung volumes and to the possible stiffness

of the excised lung tissues. Recently, data have been obtained by Jackson et al. in anesthetized and paralysed dogs in a 0 to 64 Hz range. The monotonous increase of the resistance with frequency is confirmed by their measurements. The frequency dependence of the impedance is in qualitative agreement with the results of our calculations.

The modifications of the frequency dependence of the resistance caused by bronchial obstruction was first described by Grimby et al. [21]: in patients with obstructive lung disease. The decrease of the respiratory resistance with increasing frequencies (3–9 Hz), have been interpreted as an effect of an uneven distribution of the mechanical properties of the lung. But the true nature of the unevenness could not be elucidated. Later on, the slope of the resistance, in a low frequency range, has been taken as an index characterizing the degree of obstructive lung disease. An interesting result of our modellization of airflow in the bronchial tree is that the rise of the absolute value of the slope in the 3 to 9 Hz range, might not be an early indication of bronchial obstruction: depending on the value of the lung tissue resistances, the raise of the resistance slope may occur at an earlier as well as at a later stage of small airways obstruction. Furthermore this raise is observed only at degrees of obstruction varying in a limited range: when the smallest airway diameter is diminished below a certain limit, the simulation shows that the resistance and its slope suddenly drop, thus suggesting the inability of the slope index to quantify severe bronchial obstruction. The simulation indicates that a larger frequency range should be considered in order to detect obstruction at an early stage and that high frequency modifications of the acoustical impedance should be better appreciated.

## REFERENCES

- [1] Office Federal de la Statistique: (Annuaire statistique de la Suisse).
- [2] Institut fuer Medizinische Statistik (IMS) Zoug.
- [3] Rapports annuels et statistiques concernant les diagnostics médicaux de la VESKA.
- [4] R. PESLIN and J. J. FREDBERG, "Oscillation mechanics of the respiratory system" to be published in the *Handbook of Physiology* (American Physiological Society).
- [5] T. J. PEDLEY, *Pulmonary fluid dynamics*, Ann. Rev. Fluid Mech. 9 (1977) 229.
- [6] T. J. PEDLEY, R. C. SCHROETER, and M. F. SUDLOW, *Flow and pressure drop in systems of repeatedly branching tubes*, J. Fluid Mech. 46 (1971) 365.
- [7] A. B. DUBOIS, A. W. BRODY, D. H. LEWIS, and B. F. BURGESS, *Oscillation mechanics of lungs and chest in man*, J. Appl. Physiol. 8 (1956) 587–594.
- [8] A. K. BOUTALEB, "L'approche de Volterra–Wiener dans la modélisation du système respiratoire et analyse décislonnelle en soins intensifs," Thèse EPFL Lausanne 1984.
- [9] J. J. FREDBERG and A. HOENIG, *Mechanical response of the lungs at high frequencies*, J. Biomech. Engineering 100 (1978) 57–66.
- [10] J. J. FREDBERG and J. MEAD, *Impedance of intrathoracic airway models during low frequency periodic flow*, J. Appl. Physiol.: Respirat. Environ. Exercise Physiol. 47 (1979) 347–351.
- [11] J. J. FREDBERG and J. A. MOORE, *The distributed response of complex branching duct networks*, J. Acoust. Soc. Am. 63(3) (1978) 954–961.
- [12] D. C. WINTER and R. L. PIMMEL, *The influence of reflection artifacts on apparent phase velocity measurements in the trachea*, Ann. Biomed. Eng. 8 (1980) 29.
- [13] H. FRANKEN, J. CLEMENT, M. CAUBERGHS, and K. P. VAN DE WOESTIJNE, *Oscillating flow of a viscous compressible fluid through a rigid tube: A theoretical model*, IEEE Trans. on Biom. Eng. BME-28 5 (1981) 416.
- [14] A. H. BENADEF *On the propagation of sound waves in a cylindrical conduit*, J. Acoust. Soc. Am. 44 (1968) 616.
- [15] P. M. MORSE and K. U. INGARD, *Theoretical acoustics*, MacGraw-Hill (1968) 475.
- [16] E. WEIBEL, "Morphometrics of the lung" in *Handbook of Physiology* (1963) Springer Verlag.

- [17] K. HORSEFIELD and G. CUMMING, *Morphology of the bronchial tree in man*, J. Appl. Physiol. 24(3) (1968) 373.
- [18] J. NAGELS, F. J. LANDSER, L. VAN DER LINDEN, J. CLEMENT, and K. P. VAN DE WOESTIJNE, *Mechanical properties of lungs and chest wall during spontaneous breathing*, J. Appl. Physiology 49 (1980).
- [19] H. VAN BRABANDT, M. CAUBERGHS, E. VERBEKEN, P. MOERMAN, J. M. LAUWERYNS, and K. P. VAN DE WOESTIJNE, *Partitioning of pulmonary impedance in excised human and canine lungs*, J. Appl. Physiology 55(6) (1983) 1733.
- [20] K. E. FINUCANE, S. V. DAWSON, P. D. PHELAN, and J. MEAD, *Resistance of intrathoracic airways of healthy subjects during periodic flow*, J. Appl. Physiology 38 (1975) 517-530.
- [21] G. GRIMBY, T. TAKASHIMA, W. GRAHAM, P. MACKLEM, and J. MEAD, *Frequency dependence of flow resistance in patients with obstructive lung disease*, J. Clin. Invest. 47 (1968) 1455.
- [22] A. JACKSON, J. W. WATSON, and M. I. KOTLIKOFF, *Respiratory system, lung and chest wall impedances in anesthetized dogs*, J. Appl. Physiology 57(1) (1984) 34.